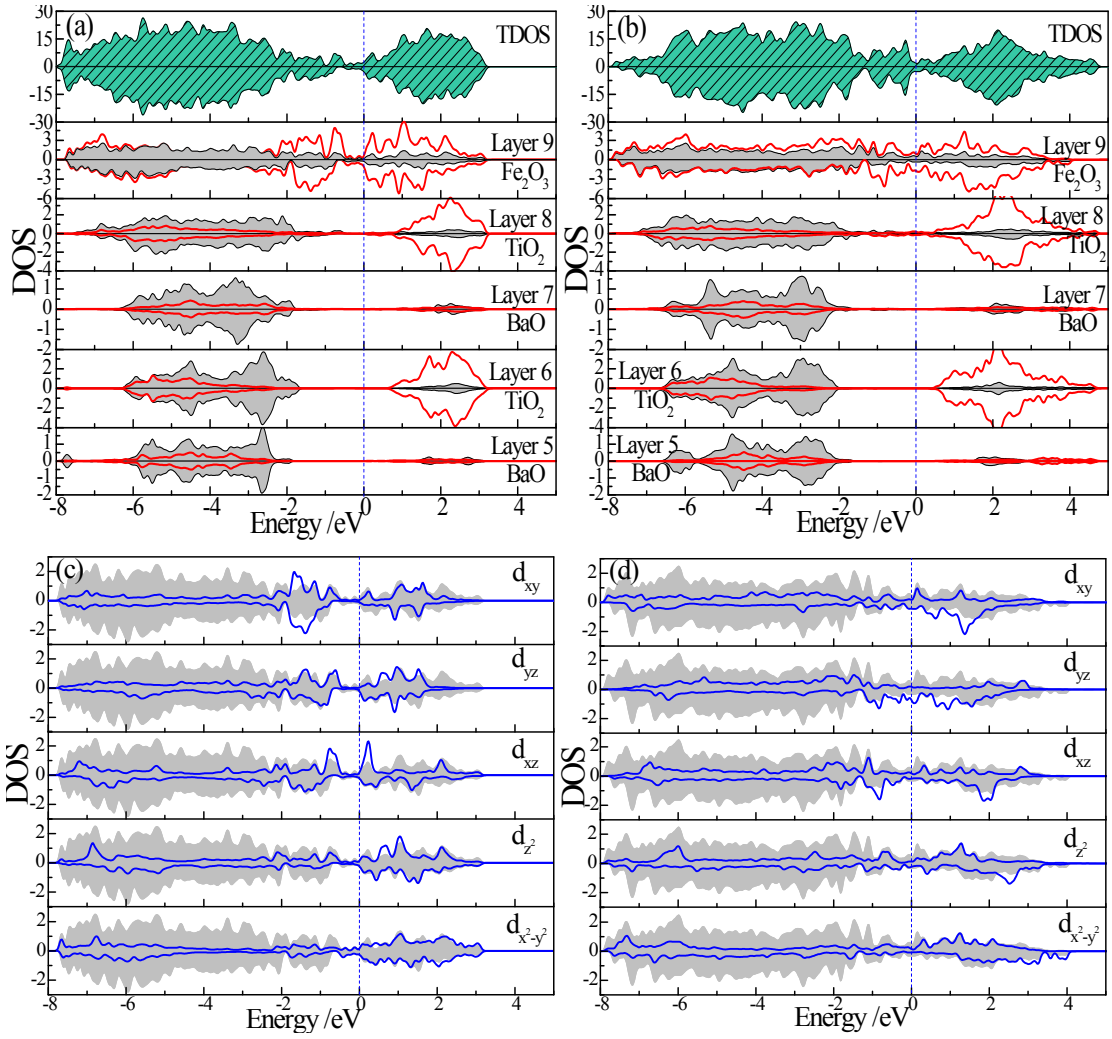

Fig. S1 The total density of states (TDOS) and the layer-resolved partial DOS (PDOS) at the Fe/TiO_2 interface of the monolayer hematene/BTO heterostructure for (a) the −*P* case; (b) the +*P* case. The orbital-resolved DOS of the Fe-3*d* (blue-solid line) and O-2*p* (shadow) states at the Fe/TiO_2 interface of the monolayer hematene/BTO heterostructure for (c) the −*P* case and (d) the +*P* case.

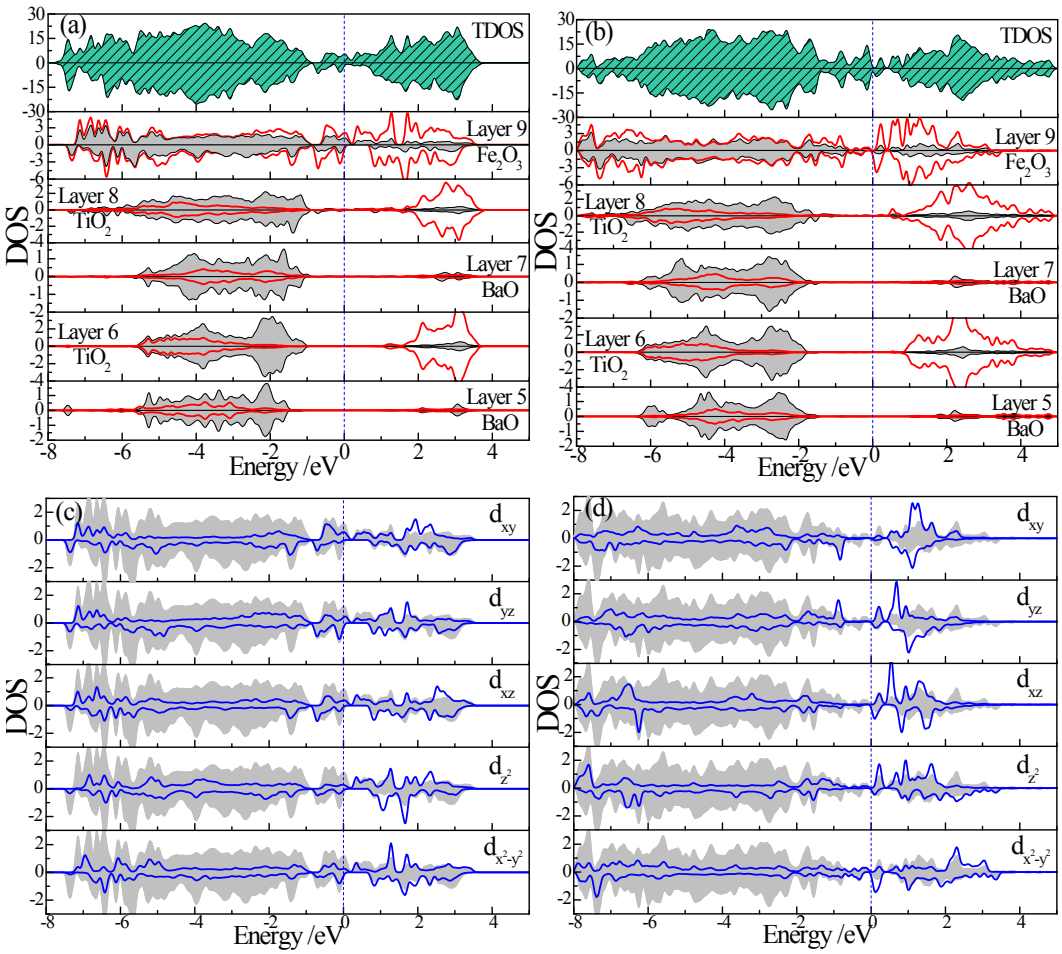

Fig. S2 The total density of states (TDOS) and the layer-resolved partial DOS (PDOS) at the O/TiO_2 interface of the monolayer hematene/BTO heterostructure for (a) the −*P* case; (b) the +*P* case. The orbital-resolved DOS of the Fe-3*d* (blue-solid line) and O-2*p* (shadow) states at the O/TiO_2 interface of the monolayer hematene/BTO heterostructure for (c) the −*P* case and (d) the +*P* case.

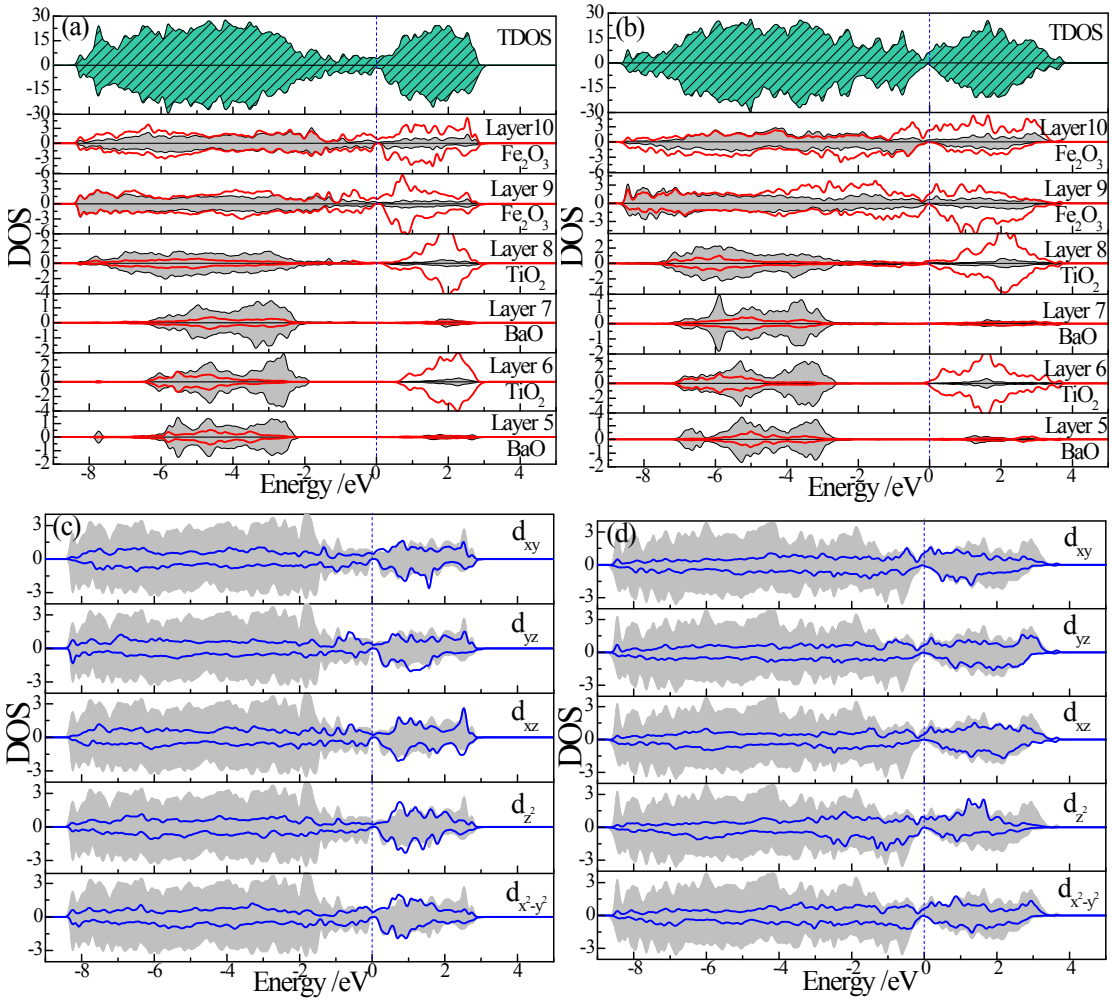

Fig. S3 The total density of states (TDOS) and the layer-resolved partial DOS (PDOS) at the Fe/TiO_2 interface of the bilayer hematene/BTO heterostructure for (a) the −*P* case; (b) the +*P* case. The orbital-resolved DOS of the Fe-3*d* (blue-solid line) and O-2*p* (shadow) states at the Fe/TiO_2 interface of the bilayer hematene/BTO heterostructure for (c) the −*P* case and (d) the +*P* case.

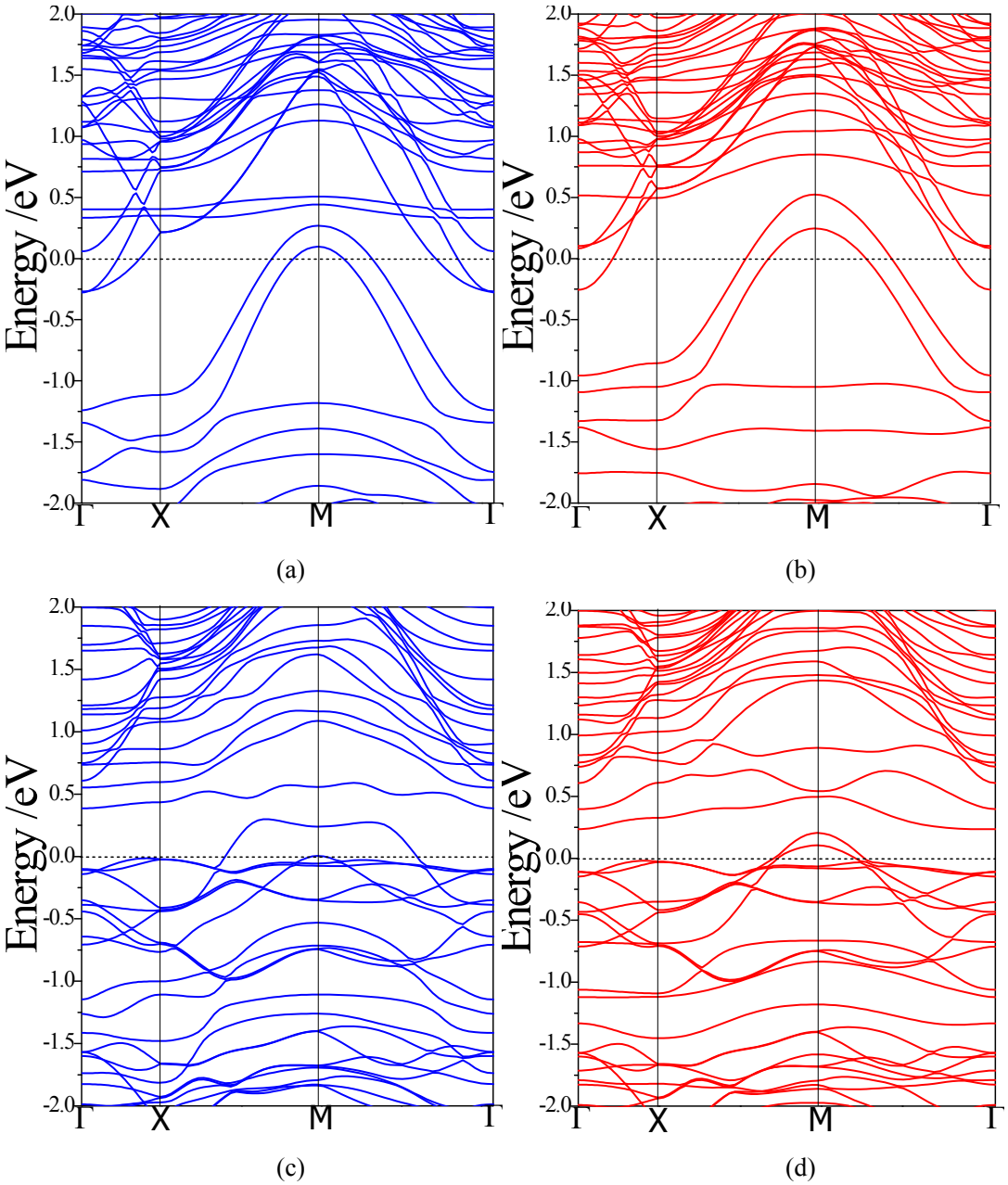

Fig. S4 The band structures of the monolayer hematene/BTO heterostructure with the Fe/TiO_2 terminated interface for (a) the spin-up channel at the −*P* case; (b) the spin-down channel at the −*P* case; (c) the spin-up channel at the +*P* case; and (d) the spin-down channel at the +*P* case.

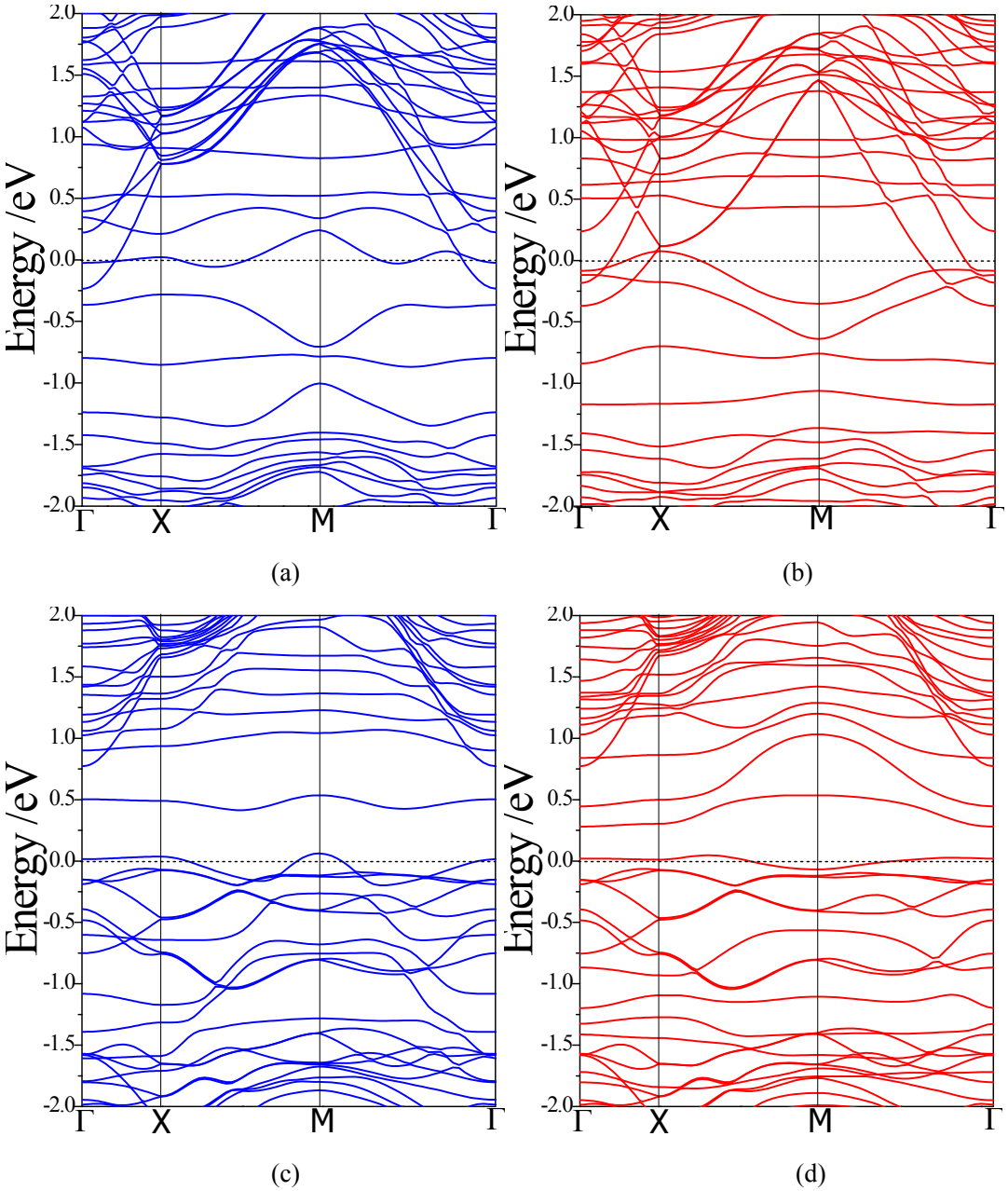

Fig. S5 The band structures of the monolayer hematene/BTO heterostructure with the O/TiO_2 terminated interface for (a) the spin-up channel at the −*P* case; (b) the spin-down channel at the −*P* case; (c) the spin-up channel at the +*P* case; and (d) the spin-down channel at the +*P* case.

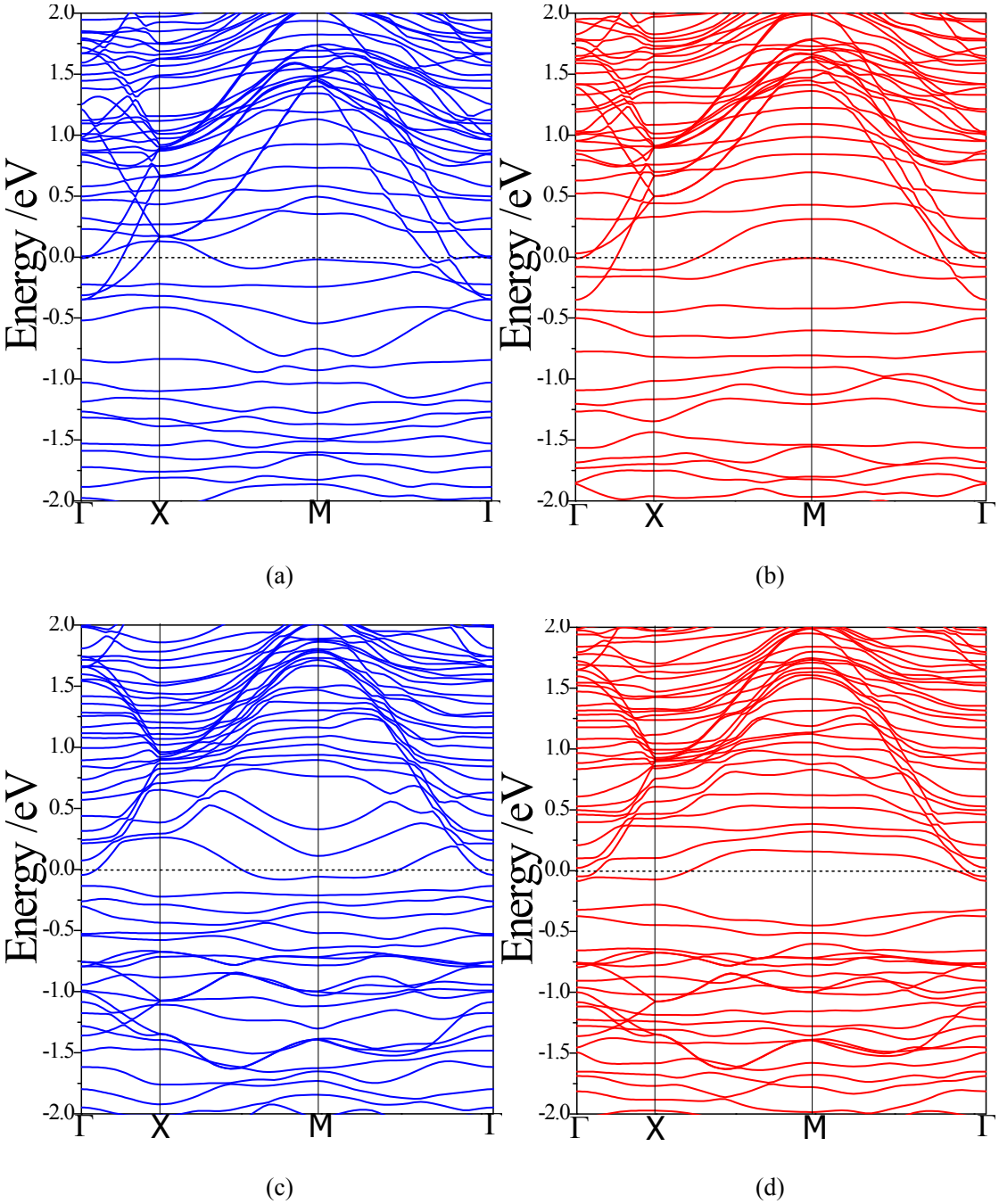

Fig. S6 The band structures of the bilayer hematene/BTO heterostructure with the Fe/TiO_2 terminated interface for (a) the spin-up channel at the −*P* case; (b) the spin-down channel at the −*P* case; (c) the spin-up channel at the +*P* case; and (d) the spin-down channel at the +*P* case.

Table S1 The calculated ground-state lattice constants *a*, *b*, and *c*, together with the magnetic moment *m* per Fe atom of the α-Fe_2O_3 bulks.

	a (Å)	b (Å)	c (Å)	m (μ_B)
This work	5.052	5.052	13.908	3.95
Expt. [1]	5.034	5.034	13.732	4.22
Calc. [2]	5.025	5.025	13.671	3.39
Calc. [3]	5.050	5.050	13.900	4.14 [4]
Calc. [5]	5.044	5.044	13.739	4.15
Expt. [6]	5.032	5.032	13.739	4.16 [7]
Expt. [8]	5.029	5.029	13.730	3.48 [9]
Calc.[10]	5.024	5.024	13.658	4.23
Expt. [11]	5.036	5.036	13.749	4.6-4.9 [12, 13]

References

[1] A. H. Hill, F. Jiao, P. G. Bruce, A. Harrison, W. Kockelmann and C. Ritter, *Chem. Mater.*, 2008, **20**, 4891-4899.

[2] X. G. Wang, W. Weiss, Sh. K. Shaikhutdinov, M. Ritter, M. Petersen, F. Wagner, R. Schlögl and M. Scheffler, *Phys. Rev. Lett*., 1998, **81**, 1038-1041.

[3] P. Guo, X. Guo and C. G. Zheng, *Fuel*, 2011, **90**, 1840-1846.

[4] A. Kiejna and T. Pabisiak, *J. Phys. Chem. C*, 2013, **117**, 24339-24344.

[5] C. X. Xia, Y. Jia, M. Tao and Q. M. Zhang, *Phys. Lett. A*, 2013, **377**, 1943-1947.

[6] K. M. Rosso, S. V. Yanina, C. A. Gorski, P. Larese-Casanova and M. M. Scherer, *Environ. Sci. Technol.*, 2010, **44**, 61-67.

[7] Z. D. Pozun and G. Hekelman, *J. Chem. Phys.*, 2011, **134**, 224706.

[8] L. Pauling and S. B. Hendricks, *J. Am. Chem. Soc.*, 1925, **47**, 781-790.

[9] G. Rollmann, A. Rohrbach, P. Entel and J. Hafner, *Phys. Rev. B*, 2004, **69**, 165107.

[10] N. Y. Dzade, A. Roldan and N. H. de Leeuw, *Minerals*, 2014, **4**, 89-115.

[11] S. Kment, F. Riboni, S. Pausova, L. Wang, L. Wang, H. Han, Z. Hubicka, J. Krysa, P. Schmuki and R. Zboril, *Chem. Soc. Rev.*, 2017, **46**, 3716-3769.

[12] J. Coey and G. Sawatzky, *J. Phys. C*, 1971, **4**, 2386-2407.

[13] E. Kren, P. Szabo and G. Konczos, *Phys. Lett.*, 1965, **19**, 103-104.